Supporting Information

Targeted perfusion adsorption for hyperphosphatemia using Mixed Matrix Microspheres (MMMs) encapsulated NH₂-MIL-101(Fe)

Wenhui Chen [a,b], Qiu Han [a], Yang Liu [a,c], Yiwen Wang [a,c], Fu Liu [a,c] *

a Key Laboratory of Marine Materials and Related Technologies, Zhejiang Key Laboratory of Marine Materials and Protective Technologies, Ningbo Institute of Materials Technology & Engineering, Chinese Academy of Sciences, No. 1219 Zhongguan West Rd, Ningbo 315201, China

b Nano Science and Technology Institute, University of Science and Technology of China, Suzhou 215000, China

c University of Chinese Academy of Sciences, 19 A Yuquan Rd, Shijingshan District, Beijing 100049, China

*Corresponding author. Tel/Fax: +86-574-86325963

E-mail: fu.liu@nimte.ac.cn (Fu Liu)
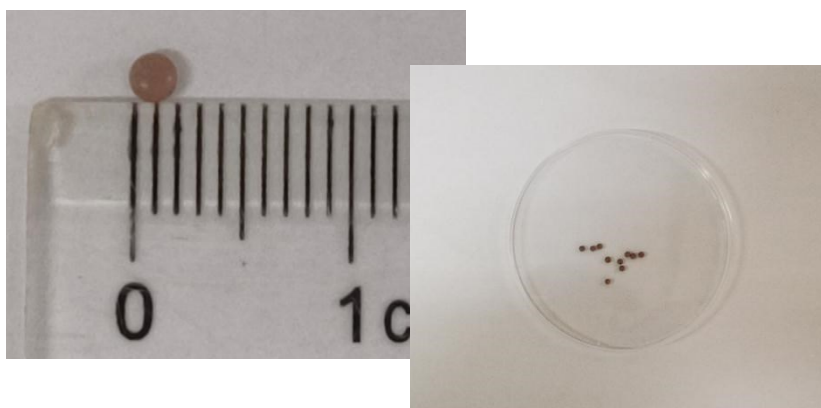
The supplementary file includes:

Fig. S1. Digital pictures of MMMs.

Fig. S2. Dynamic contact angle of MMMs and PSF microspheres.

Fig. S3. Effect of S/L ratio on the phosphate adsorption to NH_2-MIL-101(Fe) in water (C_0 = 50 mg L^{-1}) at 25°C.

Fig. S4. SEM images and element distribution after surface (a and a') and cross-section (b and b') adsorption.

Fig. S5. Zeta potential of NH_2-MIL-101(Fe).

Fig. S6. BSA adsorption onto the MMMs.

Text. S1. The pseudo-first-order and pseudo-second-order equation.

Text. S2. The Langmuir and Freundlich model.

Table S1. Phosphate adsorption capacities of various adsorbents.

Table S2. Molecular weight and molecular size of urea, creatinine, lysozyme, phosphate.

Table S3. The Lorentzian peak shape fitting parameters for O 1s XPS peak of NH_2-MIL-101(Fe) before and after phosphate adsorption.
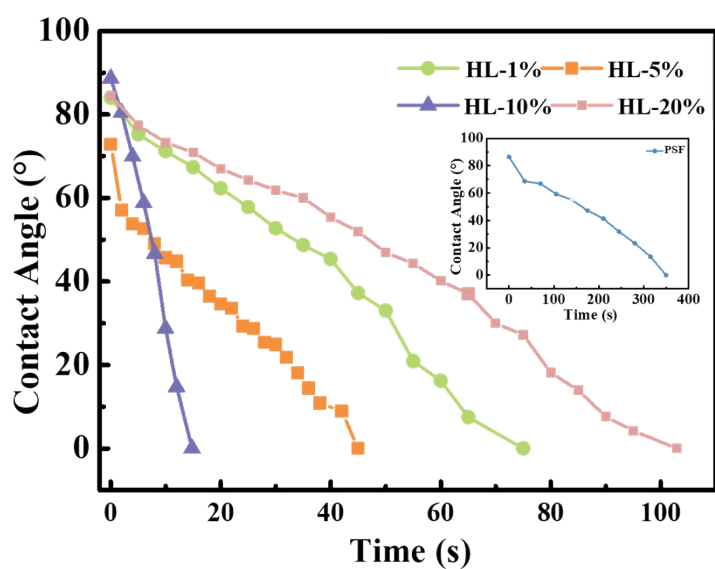
Fig. S1. Digital pictures of MMMs.

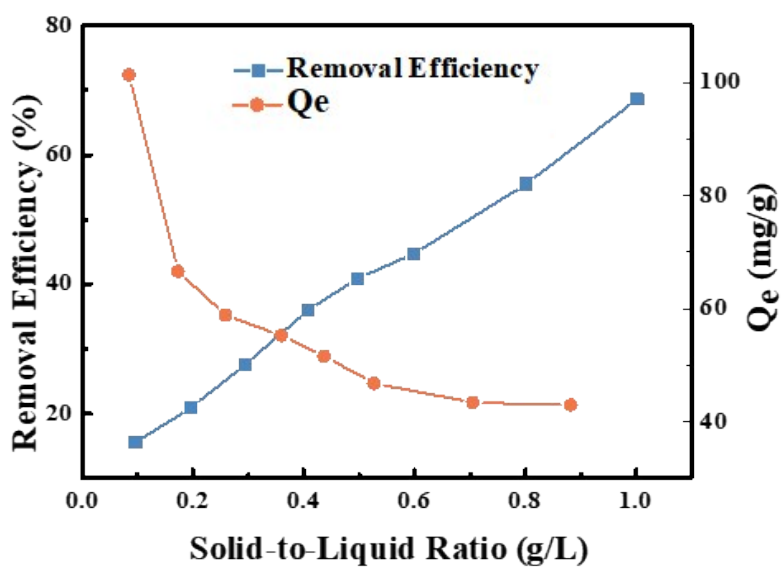**Fig. S2.** Dynamic contact angle of MMMs and PSF microspheres.

Fig. S3. Effect of S/L ratio on the phosphate adsorption to NH_2-MIL-101(Fe) in water $(C_0 = 50$ mg $L^{-1})$ at 25°C.
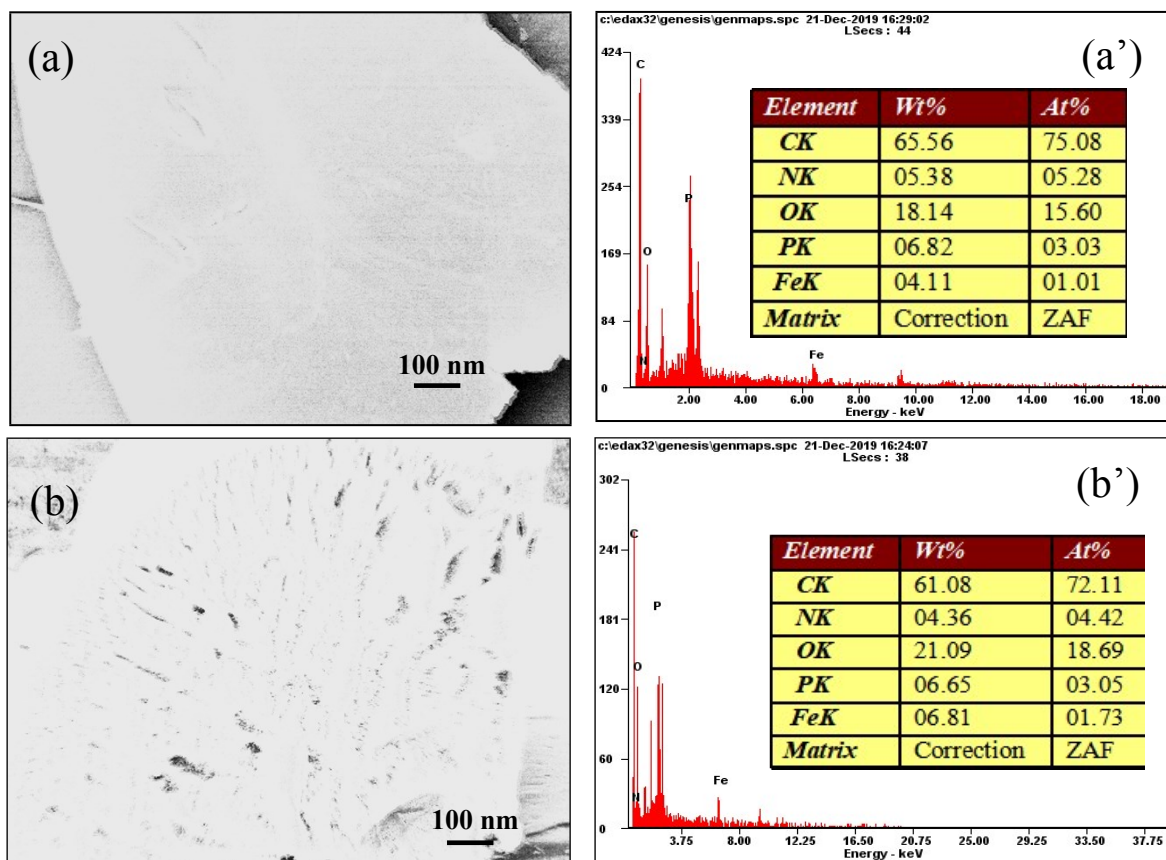
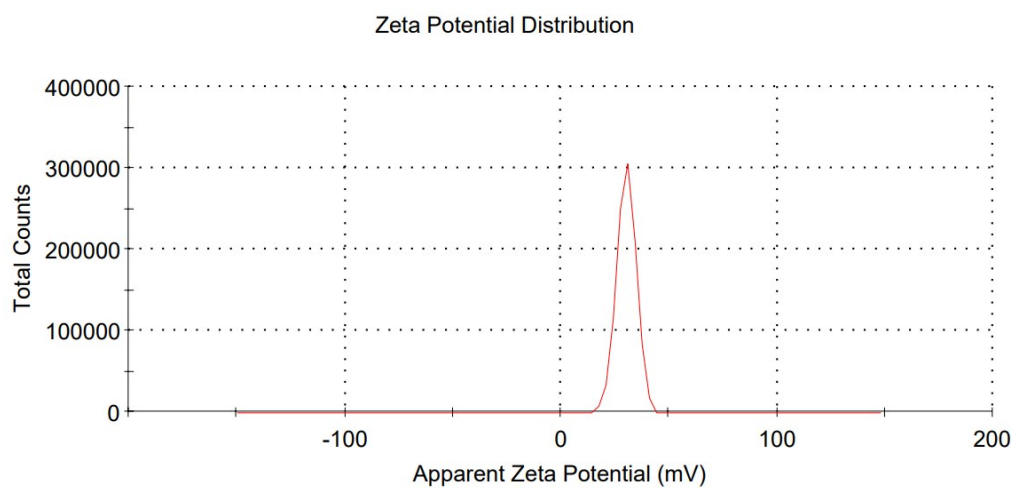**Fig. S4.** SEM images and element distribution after surface (a and a') and cross-section (b and b') adsorption.

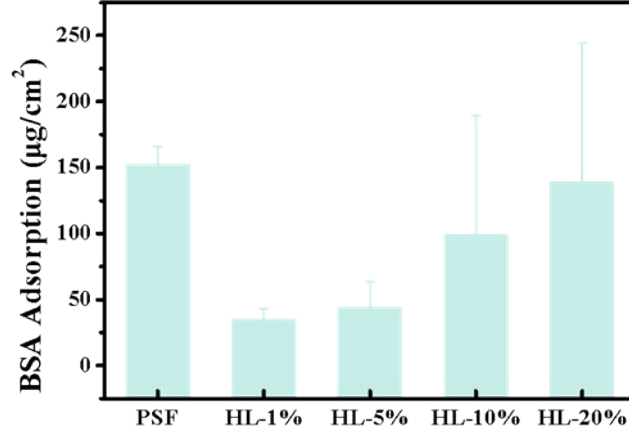**Fig. S5.** Zeta potential of NH_2-MIL-101(Fe).

Fig. S6. BSA adsorption onto the MMMs.

Text. S1

The pseudo-first-order equation:

$$\ln (Q_e - Q_t) = \ln Q_e - k_1 t$$

The pseudo-second-order equation:

$$\frac{t}{Q_t} = \frac{1}{K_2 Q_e^2} + \frac{t}{Q_e}$$

Where k_1 and k_2 are the pseudo-first-order and pseudo-second-order rate constant, Q_e (mg/g) is the adsorption capacity coefficient at equilibrium time; Q_t (mg/g) is the amount adsorbed per unit weight of sorbent at t time.

Text. S2

The Langmuir model:

$$Q_e = Q_m K_L \frac{C_e}{1 + K_L C_e}$$

The Freundlich model:

$$Q_e = K_F C_e^{1/n}$$

Q_e (mg/g) is the adsorption capacity coefficient at equilibrium time; Q_m (mg/g) is the maximal adsorption capacity in Langmuir model; C_e (mg/L) is the equilibrium concentration; K_F [(mg/g) (L/mg)$^{1/n}$] is the Freundlich capacity coefficient, and $1/n$ is isotherm curvature.

Table S1. Phosphate adsorption capacities of various adsorbents.

Adsorbent	Adsorption capacity (mg/g)	Ref
Fe-Cu binary oxides	35.2	1
La-doped ordered mesoporous hollow silica spheres	47.89	2
activated carbon nanofiber (ACF-ZrFe)	26.3	3
graphene nanosheets (GNS) supported lanthanum hydroxide (LaOH)	41.96	4
lanthanum oxide decorated graphene composite	82.6	5
β-FeOOH/GO	45.2	6
MWCNTs-COOH-La	48.02	7
Weak-base resin	61.38	8
UiO-66	85	9
UiO-66-NH$_2$	92	9
NH$_2$-MIL-101(Fe)	62.38	This Study

Table S2. Molecular weight and molecular size of urea, creatinine, lysozyme and phosphate.

Uremic Toxis	MW (g/mol)	Molecular size (nm)
Urea	60.056	0.36
Creatinine	113.12	0.54
Lysozyme	895.9	3 x 4.5
Phosphate	94.971	0.23

Table S3. The Lorentzian peak shape fitting parameters for O 1s XPS peak of NH$_2$-MIL-101(Fe) before and after phosphate adsorption.

Sample	Peak	Position BE (eV)	Area (cps eV)	percent （%）
NH$_2$-MIL-101(Fe)	Fe-O-Fe	529.4	1767.4	22.5
	Fe-OH	530.3	4526.5	57.5
	O-C=O	531.6	1574.7	20
NH$_2$-MIL-101(Fe)/Phosphate	Fe-O-Fe	529.3	3243.8	23.1
	Fe-OH/Fe-O-P/P=O	530.2	5977.8	42.5

P-OH	531.2	2716.4	19.3
O-C=O	531.9	2134	15.2

References

1 G. L. Li, S. Gao, G. Zhang, X. W. Zhang, *Chem. Eng. J.*, 2014, **235**, 124-131.

2 W. Y. Huang, Y. Zhu, J. P. Tang, X. Yu, X. L. Wang, D. Li, Y. M. Zhang, *J. Mater. Chem. A*, 2014, **2**, 8839-8848.

3 W. Xiong, J. Tong, Z. Yang, G. G. Zeng, Y. Y. Zhou, D. B. Wang, P. P. Song, R. Xu, C. Zhang, M.Cheng, *J. Colloid Interface Sci.*, 2017, **493**, 17-23.

4 L. Zhang, Y. Gao, Q. Zhou, J. Kan, Y. Wang, *Water Air & Soil Pollution*, 2014, **225**, 1967.

5 M. L. Chen, C. B. Huo, Y. K. Li, J. H. Wang, *ACS Sustainable Chem. Eng*, 2016, **4**, 1296-1302.

6 D. Harijan, V. Chandra, *J. Water Process. Eng.*, 2017, **19**, 120-125.

7 E. Zong, X. Liu, J. Wang, S. X. Yang, J. H. Jiang, S. Y. Fu, *J Mater Sci*, 2017, **52**, 7294-7310.

8 M. R. Awual, A. Jyo, *Desalination*, 2011, **281**, 111-117.

9 K. A. Lin, S. Y. Chen, A. P. Jochems, *Mater Chem Phys*, 2015, **160**, 168-176.